RZ 3389 (# 93435) 12/17/01
Electrical Engineering 7 pages

# Research Report

## Perpendicular and Longitudinal Recording: A Signal-Processing and Coding Perspective

Roy D. Cideciyan, Evangelos Eleftheriou, and Thomas Mittelholzer

IBM Research
Zurich Research Laboratory
8803 Rüschlikon
Switzerland

# Perpendicular and Longitudinal Recording: A Signal-Processing and Coding Perspective

Roy D. Cideciyan, Evangelos Eleftheriou, and Thomas Mittelholzer

*IBM Research, Zurich Research Laboratory, 8803 Rüschlikon, Switzerland*

## Abstract

Equalization and noise prediction followed by sequence detection and postprocessing are studied for double-layer perpendicular recording channels that are corrupted by electronics and transition noise. The performance of various outer coding schemes, such as conventional Reed–Solomon (RS) codes with 8-bit and 10-bit symbols and low-density parity check (LDPC) codes, is evaluated, and a signal-processing and coding perspective is presented for both longitudinal and perpendicular recording channels. Finally, the capacity of recording channels is characterized.

## I. Introduction

Areal density improvements have been the main driving force of progress in magnetic recording technology. For the past 45 years, the areal density of disk drives has increased ten million fold, leading to a dramatic reduction in storage cost. Commercial disk drives use longitudinal recording but the rate of areal density growth in longitudinal recording is expected to slow down as we approach the superparamagnetic limit. This has increased research and development efforts in perpendicular recording, which since its inception [1], [2] has promised to achieve much higher areal densities than longitudinal recording can. Recent lab demonstrations provide a clear indication that perpendicular recording may attain ultra-high areal densities [3], [4]. Ultimately, perpendicular recording promises areal densities that are about four to five times higher than those of longitudinal recording [5], [6]. However, the engineering challenges associated with the realization of this promise are formidable [7]. A transition from longitudinal to perpendicular recording would entail changes in various drive subsystems such as head, disk, head/disk interface, servo, signal processing, coding, etc. This paper will only focus on the signal-processing and coding aspects of perpendicular recording, and offer a short-term and a long-term perspective for both longitudinal and perpendicular recording.

During the past decade several digital signal-processing techniques have been introduced into disk drives to improve the error-rate performance at ever increasing normalized linear densities. In the early nineties, partial-response class-4 (PR4) shaping in conjunction with maximum likelihood sequence detection [8] replaced analog peak detection, and paved the way for future applications of advanced coding and signal-processing techniques. At higher normalized linear densities, generalized partial-response polynomials with real coefficients reduce noise enhancement at the output of the equalizer. In particular, channel polynomials of the form $(1-D)P(D)$ and $(1-D^2)P(D)$, where $P(D) = 1 + \sum_{i=1}^{L} p_i D^i$ is a finite impulse response noise-whitening filter with real coefficients $p_i$, are significant in practice. Generalized partial-response channels in conjunction with sequence detection give rise to noise-predictive maximum likelihood (NPML) systems [9]–[11]. Multiparity linear inner codes deliver additional improvements in performance when decoded by a postprocessor that follows the NPML detector and utilizes some form of reliability information [12]–[16]. Currently, a 16-state NPML detector for a generalized partial-response channel with a first-order null at DC followed by a postprocessor represents the de facto industry standard.

Outer error control codes have played an important role in achieving high data integrity in recording systems. In disk drives, interleaved byte-oriented Reed–Solomon (RS) coding is currently the standard outer coding scheme. In the future, RS symbols with more than eight bits, longer sector sizes, and advanced schemes based on Turbo or LDPC coding and iterative decoding [17], [18] promise to approach the ultimate information-theoretic limit, which is known as the capacity [19].

The perpendicular recording channel can also be viewed as a noisy communication channel with binary inputs. As in longitudinal recording, the dominant noise sources are transition and electronics noise. Note that DC erase noise can be considered as part of the electronics noise. The classical communication channel perspective can therefore be applied to study equalization, detection, inner and outer coding strategies, and the ultimate information-theoretic limits of perpendicular recording. Moreover, this viewpoint allows a comparison of longitudinal and perpendicular recording based on the performance measures of signal-to-noise ratio (SNR), error rate, and capacity.

The paper is organized as follows. In Section II, we describe the recording channel model. In Section III, we study equalization targets and noise whitening for perpendicular recording from a minimum mean-square error (MMSE) viewpoint. In Section IV, we analyze the structure of error events at the output of an NPML detector to select the appropriate postprocessing schemes. In Section V, we compare longitudinal and perpendicular recording using RS outer codes. In Section VI, we compare longitudinal and perpendicular recording using LDPC outer codes. In Section VII, we characterize the capacity of the longitudinal and the perpendicular recording channel with binary, independent and identically distributed (i.i.d.) inputs using the Shamai–Laroia (SL) conjectured lower bound [20].

## II. Recording Channel Model

Figure 1 shows the recording model used. It is characterized by the channel impulse response $g(t)$, the low-pass filter (LPF) at the receiver, the equalizer, and the noise predictor. Note that $g(t) = h(t) - h(t-T)$, where $h(t)$ is the isolated transition response.

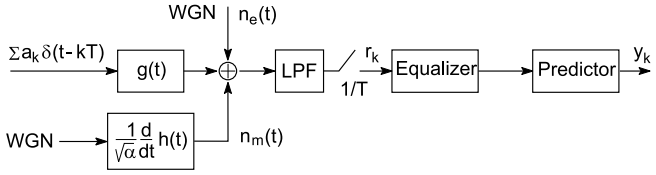


Fig. 1. Recording channel model.

An analytic frequency domain approximation of the transition response $h(t)$ for longitudinal and perpendicular recording has been presented in [7]. For a thin magnetic medium, a small gap head and sharp transitions, this signal model further simplifies, and the temporal Fourier transform of the transition response becomes

$$H(f) = \frac{\sinh(2\pi f(d_{\rm sh} - d)/v - j\theta + \gamma_s)}{\sinh(2\pi f d_{\rm sh}/v + (\gamma_s + \gamma_h))}, \qquad (1)$$

where $f$ is the frequency, $v$ the relative velocity between recording head and medium, $j$ the imaginary unit, $d$ the spacing from head to mid-plane of medium; $d_{\rm sh}$ is the spacing from head to soft underlayer, $\theta$ is the angle of magnetization, $\gamma_s = -(1/2)\ln((\mu_s - 1)/(\mu_s + 1))$, where $\mu_s$ is permeability of the soft underlayer, and $\gamma_h = -(1/2)\ln((\mu_h -$

$1)/(\mu_h + 1)$), where $\mu_h$ is permeability of the head shields. Furthermore, it has been assumed that $2M_r\delta\epsilon_h = 1$, where $\delta$ is the media thickness, $M_r$ the remanent magnetization, and $\epsilon_h$ the readback efficiency. In the case of longitudinal recording without a soft underlayer ($\theta = 0$, $\gamma_h = 0$, $d_{\rm sh} \gg d$), one obtains the familiar frequency response of the single-parameter Lorentzian model $H(f) = e^{-2\pi fd/v}$. To obtain an equivalent single-parameter model for perpendicular recording with a soft underlayer, it is assumed that $d_{\rm sh} = 2d$, $\mu_s = 100$ and $\mu_h = 1000$. Note that the condition $d_{\rm sh} \geq 2d$ ensures that the frequency domain transition response in the presence of a soft underlayer can be approximated at high frequencies by the Lorentzian response $e^{-2\pi fd/v}$.

The normalized linear channel density is defined as

$$D_c = \frac{2d}{B}, \tag{2}$$

where $B$ denotes the channel bit length. In the case of longitudinal recording, $D_c$ coincides with the normalized linear density $PW_{50}/T$ used in signal processing for longitudinal recording, where $PW_{50}$ is the half-amplitude pulse width of the time-domain Lorentzian response, and $T = B/v$ is the channel bit time. At a normalized channel density $D_c = 3$, Fig. 2 shows the amplitude response $|j2\pi fH(f)|$ for longitudinal (Lorentzian) and perpendicular recording. Note that both curves have essentially the same high-frequency content, and that the energy of the perpendicular response at low frequencies is about 2 dB higher than that of the longitudinal response. Furthermore, the perpendicular response has a very narrow notch at DC.

At very high recording densities, the dominant noise source for both recording modes is transition position jitter. The noise processes considered here include electronics noise and stationary transition noise [21] added to the signal at the input of the low-pass filter. Electronics noise $n_e(t)$ is generated by a white Gausian noise (WGN) source with two-sided spectral density $N_0/2$. Stationary transition noise $n_m(t)$ is generated by passing another WGN source with two-sided spectral density $N_m/2$ through a unit-energy filter with impulse response $\frac{1}{\sqrt{\alpha}}\frac{d}{dt}h(t)$, i.e.,

$$\alpha = \int_{-\infty}^{\infty} |\frac{d}{dt}h(t)|^2 dt. \tag{3}$$

In this paper, SNR is defined as the inverse of the sum of the spectral densities of the two WGN sources that generate the noise processes, i.e., SNR $= 2/(N_0 + N_m)$. Furthermore, at high normalized linear densities, the ratio of the transition noise to the total noise power at the output of the low-pass filter is closely approximated by the ratio of power spectral densities $\beta = N_m/(N_0 + N_m)$. Finally, a fifth-order Butterworth LPF with a 3 dB-cutoff frequency at the Nyquist frequency has been assumed for all simulations.

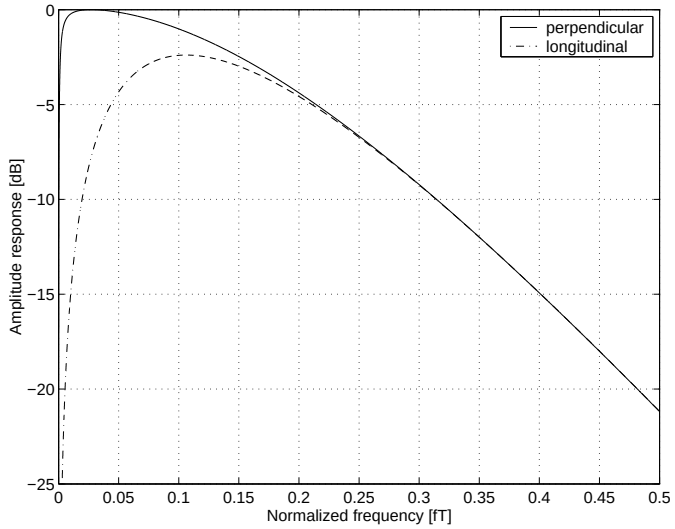


Fig. 2. Amplitude response at $D_c = 3$.

## III. Equalization and Noise Whitening

Generalized partial-response channels can be viewed as a model for the chain of signal-processing functions that include write precompensation, write driver, read/write process, preamplifier, automatic gain control, low-pass filtering, sampling, equalization, and noise whitening. The total noise at the output of the predictor is approximately white, provided that the equalizer and the predictor are sufficiently long. In the literature, see e.g. [22], [23] and [24], the double-layer perpendicular recording medium has usually been modeled without a notch at DC. However, when studying the perpendicular recording channel, assuming a spectral null at DC is important from a signal-processing viewpoint. In particular, the interesting question of how to select a generalized partial-response target that achieves a good tradeoff among various factors such as good mean squared error performance at the predictor output, reduced amount of misequalization, and low implementation complexity of equalization, prediction and detection, can only be addressed with a channel model that includes a spectral null at DC.

TABLE I
Signal processing parameters of the four cases studied.

| Case | Channel | Eqlz. target | Eqlz. taps | Pred. taps |
|---|---|---|---|---|
| I | long. | $1 - D^2$ | 10 | 2 |
| II | perp. | $1 - D^2$ | 10 | 2 |
| III | perp. | $1 + 0.75D$ | 10 | 3 |
| IV | perp. | $1 + 0.75D$ | 100 | 1 |

For the four cases listed in Table I, MMSE has been computed at the output of the predictor filter. For $\beta = 0.5$ and SNR $= 25$ dB, Fig. 3 shows the MMSE performance of these four cases as a function of $D_c$. Of the various equalization targets considered for perpendicular recording, target $1 + 0.75D$ achieved the lowest MMSE at the output of a generalized partial-response channel with memory less than or equal to four. However, as the amplitude response of the perpendicular recording channel has a notch at DC,

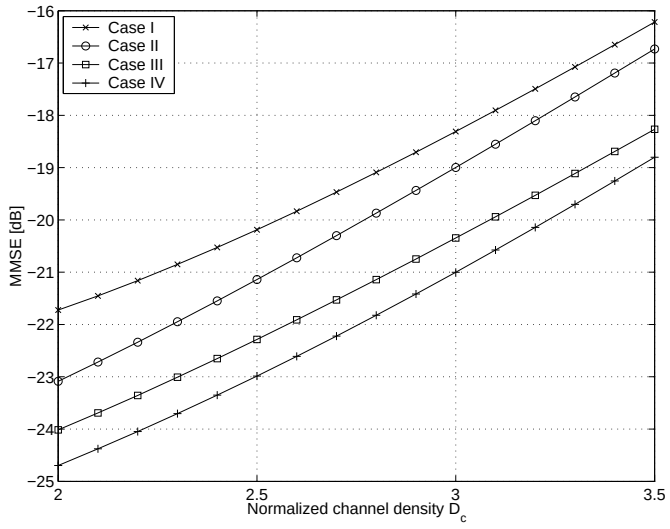


Fig. 3. MMSE vs. normalized linear density for $\beta = 0.5$.

misequalization becomes an important issue for an equalization target without a spectral null at DC, which must be carefully considered in the design of the signal-processing scheme. In fact, as seen in Fig. 3, increasing the number of taps of the $1 + 0.75D$ equalizer from 10 to 100 reduces MMSE by about 0.6 dB, and requires only one predictor tap for adequate MMSE performance.

## IV. Detection and Error Event Analysis

PR4 and extended PR4 channels, which until quite recently were the state of the art, are specified by monic polynomials with integer coefficients. At higher normalized linear densities, generalized partial-response polynomials with real coefficients provide a better match to the magnetic recording channel. The complexity of NPML detectors grows exponentially with the memory of the generalized partial-response channel. All NPML detectors for the cases specified in Table I except the one corresponding to case IV have 16 states. The detector for case IV with a memory-two generalized partial-response target has only four states. Currently, NPML detectors for a memory-four generalized partial-response target with first-order null at DC, which operate at about 1 Gbit/sec, represent the state of the art in the disk-drive industry.

The error events at the output of an NPML detector depend on the generalized partial-response target and the normalized linear channel density $D_c$. The error events at the 16-state detector output and their relative frequency of occurrence for case III in Table I are shown in Table II for three perpendicular recording channels with 50% electronics noise and 50% transition noise, i.e., $\beta = 0.5$. A shorthand notation to represent ternary error events has been used. For example, "$+-$" is used to denote the error events "$+1, -1$" and "$-1, +1$". The perpendicular recording channels operate at $D_c = 2.34$, $D_c = 2.92$, and $D_c = 3.51$, and the corresponding SNRs are 13.75, 15.25, and 17.25 dB, respectively. Furthermore, the bit error rates at the output of the NPML detector are $5.41 \times 10^{-6}$, $6.27 \times 10^{-6}$ and $6.04 \times 10^{-6}$, respectively. It can be seen that at low and moderate linear densities, the error event "$+$" is dominant, whereas at high linear densities the error event "$+-+$" occurs most often. The percentage of the error event "$+$" decreases with increasing normalized linear density, whereas the percentage of all other error events in Table II increases with increasing normalized linear density.

TABLE II
Error events at detector output.

| Error Events | $D_c = 2.34$ | $D_c = 2.92$ | $D_c = 3.51$ |
|---|---|---|---|
| $+$ | 97.79% | 61.57% | 5.64% |
| $+-$ | 1.43% | 14.80% | 24.46% |
| $+-+$ | 0.73% | 20.96% | 57.99% |
| $+-+-$ | 0.01% | 1.61% | 5.48% |
| $+-+-+$ | 0.01% | 0.90% | 4.77% |
| $+-+-+-$ | 0.00% | 0.16% | 0.97% |
| $+-+-+-+$ | 0.00% | 0.00% | 0.47% |
| $+-+-+-+-$ | 0.00% | 0.00% | 0.07% |
| $+-+-+-+-+$ | 0.00% | 0.00% | 0.10% |
| other | 0.03% | 0.00% | 0.05% |

The error event statistics in Table II indicate that at low normalized linear densities the use of a single parity postprocessing scheme that corrects the error events "$+$" would improve performance. In general, at moderate and high normalized linear densities, the use of a dual parity postprocessing scheme that corrects the error events "$+$", "$+-$", "$+-+$" and "$+-+-+$" is beneficial for both longitudinal and perpendicular recording.

## V. Reed-Solomon Code Performance

In disk drives interleaved RS outer codes are usually concatenated with inner modulation and parity check codes. The current RS symbol size is $s = 8$ and may be replaced in the short term by a larger number, e.g. $s = 10$. RS codes with $s = 10$ allow the encoding of a 512-byte sector into a single RS codeword. Therefore, the full power of error correction can be applied across the entire sector, resulting in a performance gain. The parameters of the inner and outer coding schemes that have been selected to study the performance of RS codes on longitudinal and perpendicular channels are summarized in Table III. The RS codes have a codeword length of $n$ symbols, and are used to correct $t$ symbols per codeword. A 512-byte sector is encoded into $I$ RS codewords, and symbol interleaving with depth $I$ is applied before modulation and parity check coding. Finally, cyclic redundancy check coding with few bytes of redundancy have been assumed to reduce the miscorrection probability of RS codes.

Dual parity modulation codes have been selected to study RS code performance at high normalized linear densities. Specifically, a dual parity rate-96/100 modulation/parity code has been used for RS outer codes with 8-bit symbols whereas a dual parity rate-80/84 modulation/parity inner code has been employed for RS outer codes with 10-bit symbols.

The normalized user density $D_u$ is defined by $D_u = RD_c$, where $R$ is the total code rate of the inner and outer

TABLE III
CODING PARAMETERS USED TO STUDY RS CODE PERFORMANCE.

| $s$ | $n$ | $I$ | $t$ | Inner code rate | Parity bits |
|---|---|---|---|---|---|
| 8 | 188 | 3 | 7 | 96/100 | 2 |
| 10 | 456 | 1 | 20 | 80/84 | 2 |

coding scheme. For example, the total code rate for the recording scheme with 10-bit RS symbols in Table III is $R = (80/84)(4096/4560) \approx 0.855$. For this code rate, the normalized channel densities $D_c = 2.34$, $D_c = 2.92$, and $D_c = 3.51$ in Table II translate into the normalized user densities $D_u = 2$, $D_u = 2.5$, and $D_u = 3$, respectively. Figure 4 shows the RS code performance for the four cases depicted in Table I at a normalized user density $D_u = 3$.

For each case in Table I the two outer and inner coding schemes in Table III using 8-bit and 10-bit RS symbols have been used. It can be seen that at sector failure rates of $10^{-4}$, 10-bit RS codes in all cases perform about 0.3 dB better than 8-bit RS codes do. Furthermore, perpendicular recording with an equalizer target $1 + 0.75D$ and 16-state NPML detection has a performance advantage of about 2 dB when compared to longitudinal recording with an equalizer target $1 - D^2$ and 16-state NPML detection. This performance gain is obtained because the perpendicular signal model used has an about 2 dB higher signal energy than that of the longitudinal signal model used. Finally, the PR4 target, which is extensively used in longitudinal recording, does not seem to be suited for perpendicular recording.

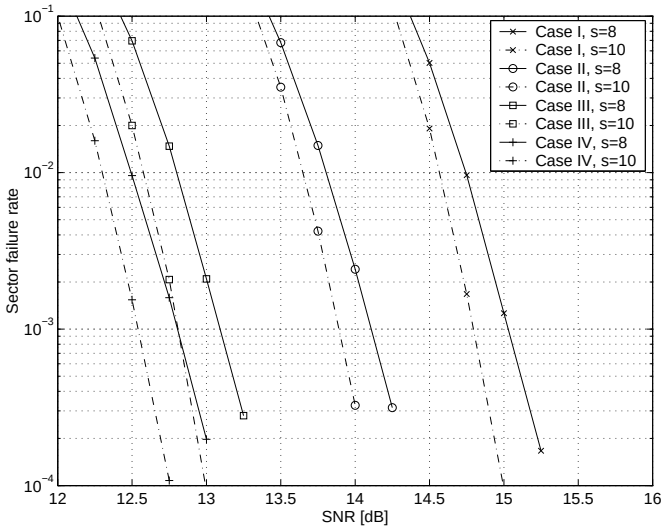


Fig. 4. Sector failure rate performance of RS codes for longitudinal and perpendicular recording channels at $D_u = 3$ with 50% electronics and 50% transition noise.

## VI. LDPC CODE PERFORMANCE

For the additive WGN (AWGN) channel, the currently most efficient coding schemes are based on turbo and LDPC codes [17], [18], [25], [26]. These schemes have also been considered as a long-term coding alternative for magnetic recording channels [27]–[32]. Such a scheme with its characteristic iterative detection and decoding section is shown in Fig. 5. A sector of binary data $\mathbf{u} = [u_1, \ldots, u_K]$ is encoded by a rate-$K/N$ LDPC encoder into a binary codeword $\mathbf{b} = [b_1, \ldots, b_N]$, and then mapped to antipodal encoded data symbols $a_n = 2b_n - 1$, $n = 1, \ldots, N$, which are written on the disk at a rate of $1/T$. For the discrete-time recording channel, we adopt the model described in Section II (see Fig. 1).

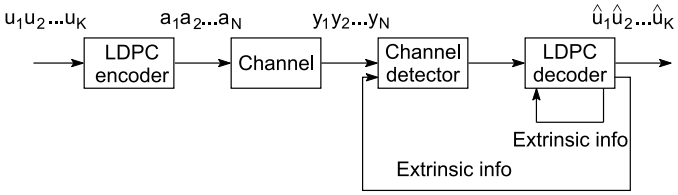


Fig. 5. System model for LDPC encoder, channel, detector, and LDPC decoder.

The key feature of the LDPC coding scheme is the iterative detection and decoding strategy, which can be described as follows. Using the channel output samples $y_1, \ldots, y_N$, the detector produces soft information about the encoded data symbols $a_n$ by taking the channel constraints into account. Making use of the code constraints, the decoder computes an estimate $\hat{u}_i$ together with (soft) extrinsic information for the encoded data symbols $a_n$. The extrinsic information may be fed back directly to the decoder or passed to the detector, depending on the detection/decoding schedule adopted.

The code selected for the simulations is a high-rate LDPC array code of length $N = 4364$ and dimension $K = 4099$, which relies on a simple deterministic construction [41] and gives state-of-the-art error performance on the AWGN channel. Furthermore, we have chosen a schedule for passing reliability information that alternates between detector and decoder. This schedule was found to be optimum in previous work [31]. Finally, the maximum number of iterations was limited to 30.

Figure 6 shows the bit and sector failure probabilities of the rate-4099/4364 LDPC code for longitudinal and perpendicular recording channels with a mixture of 50% electronics and 50% transition noise. The SL bound (SLB) on the information rate of longitudinal and perpendicular recording channels, which serves as an information-theoretic benchmark presented in the next section, is also shown in Fig. 6.

The two right-most curves in Fig. 6 show the sector-failure (solid) and bit-error probabilities (dashed) of the longitudinal recording channel with a 10-tap equalizer and a 16-state NPML target of the form $(1 - D^2)(1 + p_1 D + p_2 D^2)$. At BER $= 10^{-5}$, the code is about 1.5 dB away from the SL bound. There is a similar SNR gap for the perpendicular recording channel with a 100-tap equalizer and a detector target $(1 + 0.75D)(1 + p_1 D + p_2 D^2 + p_3 D^3)$ as illustrated by the two left-most curves in Fig. 6. When reducing the number of equalizer taps to 10, there is a performance loss of 0.35 dB. If the 16-state detector target is based on PR4, an additional loss of about 0.55 dB occurs.

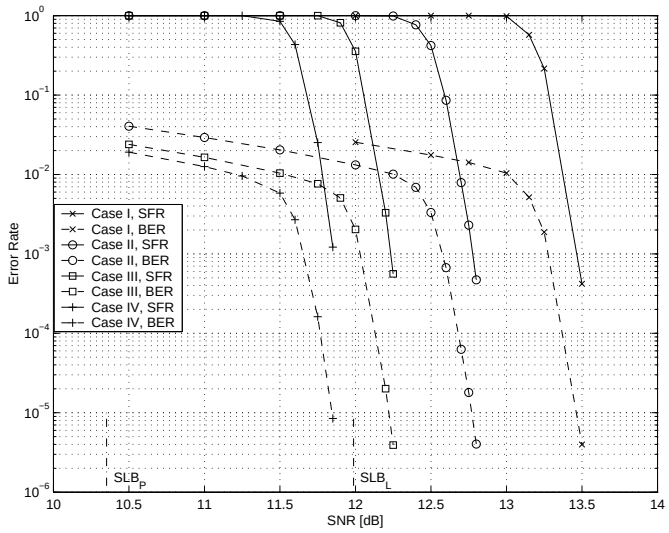


Fig. 6. Bit-error rate and sector-failure rate performance (denoted as BER and SFR in the legend) of a rate $R = 4099/4364$ LDPC code for longitudinal and perpendicular recording channels at $D_u = 3$ with 50% electronics and 50% transition noise.

## VII. Performance Limits

To assess the performance limits of reliable recording, we consider an information-theoretic approach similar to [33], [34]. However, in contrast to [33], [34], where there is a big discrepancy between the lower and upper bounds on capacity, we will follow [35] and focus on information rates between a coin-tossing binary input sequence and the output of the channel. These uniform-input information rates are closely approximated by the conjectured lower bound of Shamai and Laroia for PR4, EPR4 and E$^2$PR4 channels [20], [40]. For the channel model used, we expect a similar close matching of the SL bound with the uniform-input information rate.

To apply the SL bound we transform the continuous-time recording channel into a discrete-time channel by passing the received signal through a suitable receiver filter and a sampler. Instead of the low-pass filter in Fig. 1, we choose the receiver filter $h_r(t)$ to be a noise-whitening filter followed by a filter that is matched to the resulting signal to obtain a sufficient statistics $r_k$ for the binary input signal $a_k$ [36]. The frequency response of the receiver filter is given by

$$H_r(f) = \frac{1}{\sqrt{S_n(f)}} G^*(f) \frac{1}{\sqrt{S_n(f)}}, \tag{4}$$

where $G^*(f)$ denotes the complex conjugate of the frequency response of the impulse response $g(t)$, and where the normalized spectral density of the total noise is

$$\begin{aligned} S_n(f) &= S_{n_e}(f) + S_{n_m}(f) && (5)\\ &= 1 - \beta + \frac{\beta}{\alpha} |(2j\pi f) H(f)|^2, && (6) \end{aligned}$$

with $1-\beta$ and $\beta$ specifying the balance between electronics and transition noise, respectively. The resulting discrete-time channel with binary inputs $a_k$ and real-valued outputs $r_k$ is a matched filter receiver. It has a frequency response, which is given by the folded power spectrum

$$F(\theta) \triangleq \frac{1}{T} \sum_{\ell=-\infty}^{\infty} \frac{|G((\theta+\ell)/T)|^2}{S_n((\theta+\ell)/T)}, \qquad -\tfrac{1}{2} \le \theta < \tfrac{1}{2}. \tag{7}$$

The discrete-time noise process $\{z_k\}$ of the channel has a normalized power density $S_z(\theta)$, which is given by the folded spectrum $S_z(\theta) = F(\theta)$. Note that $F(\theta)$ is real-valued and $|F(\theta)|^2/S_z(\theta) = F(\theta)$. Moreover, $F(\theta)$ is also the power spectrum of the discrete-time channel that is obtained by whitening the noise of the matched filter receiver. Thus, for Gaussian i.i.d. inputs $\{a_k\}$ with a per-symbol energy constraint $E[a_k^2] \le S_a$ and $\mathrm{SNR} = 2S_a/(N_0 + N_m)$, the information rate (in bits/channel use) is given by [37]

$$I_G(T) = \frac{1}{2} \int_{-1/2}^{1/2} \log_2(1 + \mathrm{SNR}\, F(\theta)) d\theta. \tag{8}$$

Note that $I_G(T)$ depends on the symbol duration $T$ via $F(\theta)$. The information rate for Gaussian inputs is an upper bound for the information rate $I(T)$ of i.i.d. binary inputs with the same symbol energy.

We will recall upper and lower bounds, which rely on the capacity of the binary-input AWGN channel, the capacity of which can be easily computed [38], and which for a given SNR will be denoted by $C_{\mathrm{bin}}(\mathrm{SNR})$. The well-known matched filter (MF) bound [39] is an upper bound for $I(T)$ given by

$$I_{\mathrm{MF}}(T) = C_{\mathrm{bin}}(\mathrm{SNR}\; E_{\mathrm{MF}}), \tag{9}$$

where $E_{\mathrm{MF}} = \int_{-1/2}^{1/2} F(\theta) d\theta$ is the energy of the matched filter. Furthermore, we state the conjectured SL lower bound, which was shown to be surprisingly tight [20]:

$$I_{\mathrm{SL}}(T) = C_{\mathrm{bin}}(2^{2I_G(T)} - 1). \tag{10}$$

Figure 7 shows these bounds for longitudinal and perpendicular recording at the normalized linear density $D_c = 3.2$ with 50% electronics and 50% transition noise.

When keeping the track width constant, the figure of interest is what will be referred to as the *lineal information rate*

$$I(T)\; D_c \qquad [\text{bits/ unit time}], \tag{11}$$

which allows one to compare information rates and, in particular, capacities at different normalized linear densities $D_c$ [34].

It is illustrative to translate the above bounds into the SNR domain by fixing some code rate $R$ and finding the information-rate achieving SNR, i.e., the SNR such that $I(T) = R$. We consider these bounds as a function of normalized linear user density $D_u$, i.e., using the upper and lower bounds (9) and (10), we determine lower and upper bounds on the SNR required to achieve a given lineal information rate

$$D_u = I(T) D_c.$$

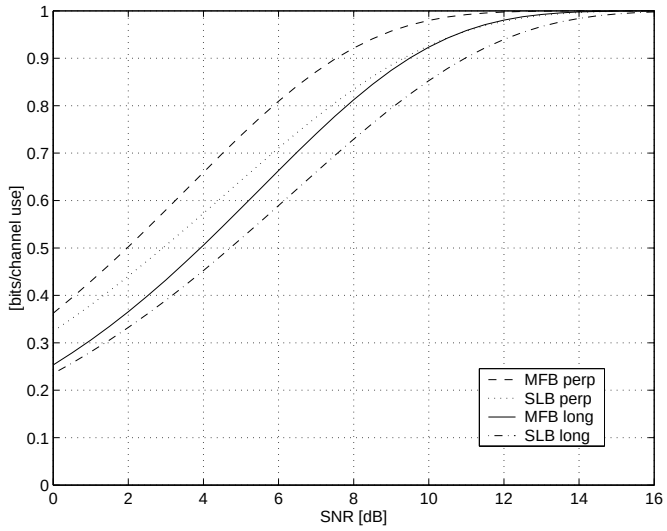


Fig. 7. Matched filter upper bound (MFB) and SL conjectured lower bound (SLB) on information rate at $D_c = 3.2$ and with a 1 : 1 blend of electronics and transition noise for longitudinal and perpendicular recording.

In Fig. 8 we have selected the coding rates $R = 4099/4364$ and 0.855, which pertain to the LDPC code and the concatenated modulation/parity and RS code used in the simulations. In Fig. 8, the two top curves (dashed) show the SL bound of longitudinal recording for the two rates of interest. The next two curves below (dotted) correspond to the MF bound. Similarly, the remaining four curves show the SL bounds for the two rates (solid) and the MF bounds (dotted) for perpendicular recording. Assuming that the SL bound is tight, the MF bound appears to be very loose for high normalized linear densities. Note that for all curves the SNR requirement in dB is almost a linear function of the normalized linear density in the region of interest.

Furthermore, there is a roughly uniform 2 dB difference between corresponding curves for longitudinal and perpendicular recording. This approximate 2 dB difference reflects the fact that the energy of the perpendicular response is about 2 dB higher than that of the longitudinal response. As shown in the preceding sections, roughly a gain of 2 dB could be achieved using a very long equalizer and a suitable detector target. However, practical systems with a limited equalizer length might suffer from a slight performance loss.

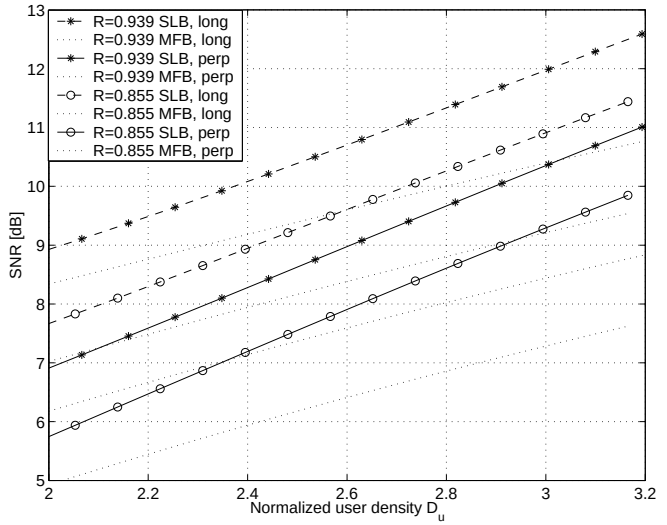


Fig. 8. MF-bound and SL-bound achieving SNR for code rates $R = 4099/4364$ and 0.855 for longitudinal and perpendicular recording with an electronics and transition noise blend of 1 : 1.

## VIII. Conclusion

We have investigated signal-processing and coding alternatives for double-layer perpendicular recording channels with a notch at DC, and compared their performance to conventional longitudinal recording. In the signal model used, the perpendicular response has an about 2 dB higher energy than that of the longitudinal response. In all the coding scenarios considered this difference in energy translated into about a 2 dB performance gain for perpendicular recording.

The target $1 + 0.75D$ has been found to be a good choice for perpendicular recording in terms of both MMSE and sector failure rate performance. Given the spectral notch at DC associated with double-layer perpendicular recording, misequalization for detection targets without a spectral null at DC needs to be properly addressed in the specification of the signal-processing architecture.

Short-term and long-term coding alternatives such as conventional RS coding with 10-bit symbols and LDPC coding have been examined. Assuming 512-byte sectors for both perpendicular and longitudinal recording at a normalized user density $D_u = 3$, it has been shown that a transition from 8-bit to 10-bit RS symbols results in an SNR gain of 0.3 dB at a sector failure rate of $10^{-4}$. For perpendicular and longitudinal recording at high normalized user densities based on 512-byte sectors, iterative decoding of LDPC codes resulted in a performance advantage of 0.75 dB and 1.5 dB, respectively, over RS decoding. Finally, it has been shown that at a sector failure rate of $10^{-4}$ the performance of LDPC coding for recording with 512-byte sectors is about 1.5 dB away from the capacity bound.

## Acknowledgment

The authors wish to express their sincere appreciation for the helpful discussions they have had with Roger Wood.

## References

[1] S. Iwasaki and Y. Nakamura, "An analysis for the magnetization mode for high density magnetic recording," *IEEE Trans. Magn.*, 13 (1977) 1272-1277.

[2] S. Iwasaki and K. Ouchi, "Co-Cr recording films with perpendicular magnetic anisotropy," *IEEE Trans. Magn.*, 14 (1978) 849-851.

[3] H. Takano et al., "Realization of 52.5 Gb/in$^2$ perpendicular recording," *J. Magn. Magn. Mater.*, 235 (2001) 241-244.

[4] Read-Rite and Samsung Electronics Record 60 Billion Bits per Square Inch Using Perpendicular Magnetic Recording, news release from Read-Rite Corp. on October 16, 2000.

[5] H. N. Bertram and M. Williams, "SNR and density limit estimates: a comparison of longitudinal and perpendicular recording," *IEEE Trans. Magn.*, 36 (2000) 4-9.

[6] R. Wood, "The feasibility of magnetic recording at 1 Terabit per Square Inch," *IEEE Trans. Magn.*, 36 (2000) 36-42.

[7] R. Wood, Y. Sonobe, Z. Jin and B. Wilson, "Perpendicular recording: the promise and the problems," *J. Magn. Magn. Mater.*, 235 (2001) 1-9.

[8] R. D. Cideciyan, F. Dolivo, R. Hermann, W. Hirt, and W. Schott, "A PRML system for digital magnetic recording," *IEEE J. Sel. Areas Commun.*, vol. 10, pp. 38-56, Jan. 1992.

[9] P. R. Chevillat, E. Eleftheriou, and D. Maiwald, "Noise-predictive partial-response equalizers and applications," in *Proc. IEEE ICC '92*, Chicago, IL, June 1992, pp. 942-947.

[10] E. Eleftheriou and W. Hirt, "Noise predictive maximum-likelihood (NPML) detection for the magnetic recording channel," in *Proc. IEEE ICC '96*, June 1996, pp. 556-560.

[11] R. Karabed and N. Nazari, "Trellis-coded noise predictive Viterbi detection for magnetic recording channels," in *Digests of The Magnetic Recording Conference (TMRC)*, Aug. 1997.

[12] T. Conway, "A new target response with parity coding for high density magnetic recording channels," *IEEE Trans. Magn.*, vol. 34, No. 4, pp. 2382-2486, July 1998.

[13] J. L. Sonntag and B. Vasic, "Implementation and bench characterization of a read channel with parity check postprocessor," in *Digests of The Magnetic Recording Conference (TMRC)*, Santa Clara, CA, August 2000.

[14] R. D. Cideciyan, J. D. Coker, E. Eleftheriou, and R. L. Galbraith, "NPML detection combined with parity-based postprocessing," in *Digests of The Magnetic Recording Conference (TMRC)*, Santa Clara, CA, August 2000.

[15] W. Feng, A. Vityaev, G. Burd and N. Nazari, "On the performance of parity codes in magnetic recording systems," in *Proc. IEEE Global Telecommun. Conf.*, pp. 1877-1881, November 2000.

[16] B. Vasic, "A graph based construction of high-rate soft decodable codes for partial response channels," in *Proc. IEEE ICC '01*, Helsinki, Finland, June 2001, pp. 2716-2720.

[17] R. G. Gallager, "Low-density parity-check code," *IRE Trans. Inform. Theory*, vol. IT-8, pp. 21-28, Jan. 1962.

[18] C. Berrou, A. Glavieux, and P. Thitimajshima, "Near Shannon limit error-correcting coding and decoding: turbo-codes," in *Proc. IEEE ICC'93*, Geneva, Switzerland, May 1993, pp. 1064-1070.

[19] C. E. Shannon, "A mathematical theory of communication," *Bell Syst. Tech. J.*, vol. 27, pp. 379-423, 1948.

[20] S. Shamai and R. Laroia, "The intersymbol interference channel: lower bounds on capacity and channel precoding loss," *IEEE Trans. Inform. Theory*, vol. 42, pp. 1388–1404, Sept. 1996.

[21] S. X. Wang and A. M. Taratorin, *Magnetic Information Storage Technology*, Academic Press, 1999.

[22] Y. Okamoto, H. Osawa, H. Saito, H. Muraoka and Y. Nakamura, "Performance of PRML systems in perpendicular magnetic recording channel with jitter-like noise," *J. Magn. Magn. Mater.*, 235 (2001) 259-264.

[23] H. Sawaguchi, Y. Nishida, H. Takano, H. Aoi, "Performance analysis of modified PRML channels for perpendicular recording systems," *J. Magn. Magn. Mater.*, 235 (2001) 265-272.

[24] M. Akamatsu, Y. Okamoto, H. Saito, H. Osawa, H. Muraoka and Y. Nakamura, "Error event analysis in perpendicular magnetic recording using double-layered medium," *J. Magn. Magn. Mater.*, 235 (2001) 475-480.

[25] D. J. C. MacKay, "Good error-correcting codes based on very sparse matrices," *IEEE Trans. Inform. Theory*, vol. 45, pp. 399-431, Mar. 1999.

[26] T. J. Richardson, A. Shokrollahi, and R. Urbanke, "Design of capacity-approaching irregular low-density parity-check codes," *IEEE Trans. Inform. Theory*, Vol. 47, No. 2, pp. 619–637, Feb. 2001.

[27] W.E. Ryan, "Performance of high rate turbo codes on a PR4-equalized magnetic recording channel," in *Proc. IEEE ICC'98*, Atlanta, GA, June 1998, pp. 947-951.

[28] W. E. Ryan, L. L. McPheters, and S. W. McLaughlin, "Combined turbo coding and turbo equalization for PR4-equalized Lorentzian channels," in *Proc. Conf. Info. Sci. Sys.*, Princeton, NJ, Mar. 1998, pp. 489-493.

[29] H. Song, R. M. Todd, and J. R. Cruz, "Low density parity check codes for magnetic recording channels," in *Proc. IEEE Intermag 2000*, Toronto, Canada, Apr. 2000.

[30] T. Souvignier, A. Friedmann, M. Oberg, P. H. Siegel, R. E Swanson, and J.K. Wolf, "Turbo decoding for PR4: parallel versus serial concatenation," in *Proc. IEEE ICC'99*, Vancouver, Canada, June 1999, pp. 1638-1642.

[31] T. Mittelholzer, A. Dholakia, and E. Eleftheriou, "Reduced-complexity decoding of LDPC codes for generalized partial-response channels," in *IEEE Trans. Magn.*, Vol. 37, No. 2, March 2001, pp. 721–728.

[32] Y. Okamoto, T. Kanaoka, H. Osawa, H. Saito, H. Muraoka, and Y. Nakamura, "Bit error rate performance of iterative decoding in a perpendicular magnetic recording channel," *IEEE Trans. Magn.*, vol. 37, No. 2, pp. 689-694, Mar. 2001.

[33] C. A. French and J. K. Wolf, "Bounds on the capacity of a peak power constrained Gaussian channel," *IEEE Trans. Magn.*, vol. 24, No. 5, pp. 2247-2262, Sep. 1988.

[34] S. W. McLaughlin and D. L. Neuhoff, "Upper bounds on the capacity of the digital magnetic recording channel," *IEEE Trans. Magn.*, vol. 29, No. 1, pp. 59-66, Jan. 1993.

[35] A. Dholakia, E. Eleftheriou, and T. Mittelholzer, "On iterative decoding for magnetic recording channels," in *Proc. of The 2nd Intl. Symp. Turbo Codes*, Brest, France, Sept. 2000, pp. 219-226.

[36] J. M. Wozencraft and I. M. Jacobs, *Principles of Communication Engineering*, Wiley, 1965.

[37] W. Hirt and J.L. Massey, "Capacity of the discrete-time Gaussian channel with intersymbol interference," *IEEE Trans. Inform. Theory*, vol. 34, pp. 380–388, May 1988.

[38] J.G. Proakis, *Digital Communications*, New York: McGraw-Hill, 1989.

[39] S. Shamai, L.H. Ozarow, and A.D. Wyner, "Information rates for a discrete-time Gaussian channel with intersymbol interference and stationary inputs," *IEEE Trans. Inform. Theory*, vol. 37, pp. 1527–1539, Nov. 1991.

[40] D. Arnold and H.-A. Loeliger, "On the Information Rate of Binary-Input Channels with Memory," *Proc. of the IEEE Intern. Conf. on Communications*, vol. 9, pp. 2692-2695, June 11-14, Helsinki, FI, 2001.

[41] J.L. Fan, "Array codes as low-density parity-check codes," *Proc. 2nd Intl. Symp. on Turbo Codes*, Brest, France, 4-7 Sept. 2000, pp. 543-546.